

---

# Injective flows for parametric hypersurfaces

---

**Marcello Massimo Negri**  
University of Basel  
marcellomassimo.negri@unibas.ch

**Jonathan Aellen**  
University of Basel  
jonathan.aellen@unibas.ch

**Volker Roth**  
University of Basel  
volker.roth@unibas.ch

## Abstract

Normalizing Flows (NFs) are powerful and efficient models for density estimation. When modeling densities on manifolds, NFs can be generalized to injective flows but the Jacobian determinant becomes computationally prohibitive. Current approaches either consider bounds on the log-likelihood or rely on some approximations of the Jacobian determinant. In contrast, we propose injective flows for parametric hypersurfaces and show that for such manifolds we can compute the Jacobian determinant exactly and efficiently, with the same cost as NFs. Furthermore, we show that for the subclass of star-like manifolds we can extend the proposed framework to always allow for a Cartesian representation of the density. We showcase the relevance of modeling densities on hypersurfaces in two settings. Firstly, we introduce a novel Objective Bayesian approach to penalized likelihood models by interpreting level-sets of the penalty as star-like manifolds. Secondly, we consider Bayesian mixture models and introduce a general method for variational inference by defining the posterior of mixture weights on the probability simplex.

## 1 Introduction

Normalizing Flows (NFs) are flexible and efficient models that allow to accurately estimate arbitrary probability distributions. The key idea is to transform a simple distribution into a complicated one through a series of bijective transformations. However, in many applications we either know that the target density lives on a certain manifold or we assume that the data was generated from some lower dimensional manifold [Cayton, 2005]. In both cases we need an injective transformation that inflates the dimensionality of the space. Unfortunately, the computation of the transformed density involves an expensive Jacobian determinant term, which makes the model computationally prohibitive. In practice, most work either consider trivial manifolds like spheres and tori [Gemici et al., 2016, Rezende et al., 2020] or approximate the Jacobian determinant term [Kumar et al., 2020, Caterini et al., 2021, Sorrenson et al., 2024], often with high variance estimators.

In this work, we propose injective flows for a general class of manifolds termed parametric hypersurfaces. Such manifolds can be parameterized by an injective transformation that inflates the dimensionality by one. We show that for such injective flows we can exactly and efficiently compute the Jacobian determinant term, with the same computational cost as NFs. For a subclass of hypersurfaces, termed star-like manifolds, we show that we can extend the proposed approach to always allow for a Cartesian representation of the density on the manifold.

Parametric hypersurfaces are relevant in variational inference settings where we are interested in learning a probability distribution subject to additional constraints. We showcase two examples for widely used Bayesian models which hint at the generality of our approach. First, we introduce a novel

Objective Bayesian approach to penalized likelihood methods. In this case the star-like manifold defines a level-set of the penalty constraint. Second, we consider Bayesian mixture models and introduce a general framework for variational inference on the mixture weights posterior. Here we constrain the posterior on the simplex, such that mixture weights always sum up to one.

We summarize the contributions of the present work as follows:

- We propose injective flows for parametric hypersurfaces and show that we can exactly and efficiently compute the associated Jacobian determinant.
- We further show that for star-like manifolds the proposed framework can be extended to allow for a Cartesian representation of the density on the manifold. Relevantly, the resulting Jacobian determinant can still be computed exactly and efficiently.
- We showcase the relevance of the proposed framework in two settings. First, we introduce a novel Objective Bayesian approach to penalized likelihood methods. Second, we introduce a general framework for posterior inference on mixture weights in Bayesian mixture models.

## 2 Preliminaries

**Density and Jacobian determinant for bijective functions** Let  $x$  be a  $d$ -dimensional random variable with unknown distribution  $p_x(x)$  and let  $z$  be a  $d$ -dimensional random variable with known base distribution  $p_z(z)$ . The key idea of NFs is to model the unknown distribution  $p_x(x)$  through a transformation  $\mathcal{T} : \mathbb{R}^d \mapsto \mathbb{R}^d$  such that  $x = \mathcal{T}(z)$ . If  $T$  is a diffeomorphism, i.e. differentiable bijection with differentiable inverse  $\mathcal{T}^{-1}$ , the change of variable formula [Rudin, 1987] allows to express  $p_x(x)$  solely in terms of the base distribution  $p_z(z)$  and  $\mathcal{T}$ :  $p_x(x) = p_z(z) |\det J_{\mathcal{T}}(z)|^{-1}$ , where  $J_{\mathcal{T}}$  is the Jacobian of the transformation  $\mathcal{T}$ . Therefore, the trade-off consists of implementing bijections with tractable  $\det J_{\mathcal{T}}$  which are still flexible enough to approximate any well-behaved distribution. One key idea is to exploit the property that, given a set of bijections  $\{\mathcal{T}^{(i)}\}_{i=1}^k$ , their composition  $\mathcal{T} = \mathcal{T}^{(k)} \circ \dots \circ \mathcal{T}^{(1)}$  is still a bijection. Since for bijections the Jacobian is a square matrix, the determinant of a composition of bijections factorizes as the product of the determinant of the individual bijections. Overall, NFs are built as

$$p_x(x) = p_z(z) |\det J_{\mathcal{T}}(z)|^{-1} \quad \text{with} \quad \det J_{\mathcal{T}}(z) = \prod_{i=1}^k \det J_{\mathcal{T}^{(i)}}(\mathbf{u}_{i-1}) \quad (1)$$

where  $\mathbf{u}_{i-1} = \mathcal{T}^{(i-1)}(\mathbf{u}_{i-2}) \circ \dots \circ \mathcal{T}^{(1)}(z)$  and  $\mathbf{u}_0 = z$ . Crucially, this property allows to efficiently model an expressive bijection  $\mathcal{T}$  by stacking simple bijective layers  $\mathcal{T}^{(i)}$  with tractable (analytical) Jacobian determinant. Typically, the Jacobian determinant of the individual bijections is made tractable by designing bijections with a triangular Jacobian, such that the determinant is simply given by the product of the diagonal entries.

**Density and Jacobian determinant for injective functions** NFs are limited by the use of bijections, which prevents modeling densities on lower dimensional manifolds. In such cases the target distribution lives on a  $m$ -dimensional manifold  $\mathcal{M}$  embedded in a  $d$ -dimensional Euclidean space  $\mathcal{M} \subset \mathbb{R}^d$ , where  $m < d$ . In order to constrain  $p_x(x)$  to live on the manifold  $\mathcal{M}$ , we rather need an injective transformation that inflates the dimensionality  $\mathcal{T}_{m \rightarrow d} : \mathbb{R}^m \mapsto \mathbb{R}^d$ . The transformed probability distribution  $p_x(x)$  can still be computed with the (more general) formula for the Jacobian determinant of injective transformations [Krantz and Parks, 2008] (Lemma 5.1.4):

$$p_x(x) = p_z(z) |\det J_{\mathcal{T}_{m \rightarrow d}}(z)|^{-1} \quad \text{with} \quad \det J_{\mathcal{T}_{m \rightarrow d}} = \sqrt{\det \left( (J_{\mathcal{T}_{m \rightarrow d}})^T J_{\mathcal{T}_{m \rightarrow d}} \right)}, \quad (2)$$

where  $J_{\mathcal{T}_{m \rightarrow d}}(z) \in \mathbb{R}^{d \times m}$  is a rectangular matrix. Note that if  $m = d$ ,  $J_{\mathcal{T}}$  is a square matrix so  $\det J_{\mathcal{T}}^T J_{\mathcal{T}} = \det J_{\mathcal{T}}^T \det J_{\mathcal{T}} = (\det J_{\mathcal{T}})^2$  and Eq. (2) reduces to Eq. (1). Crucially, since  $J_{\mathcal{T}_{m \rightarrow d}}$  is now rectangular, the Jacobian determinant can not be decomposed as the product of stacked transformations anymore, which is a crucial property of bijective flows with square Jacobian (see Eq. (1)). As a consequence, we need to explicitly compute the matrix product  $J_{\mathcal{T}_{m \rightarrow d}}^T J_{\mathcal{T}_{m \rightarrow d}}$  and then its determinant, which results in a time complexity that is  $O(m^3)$ . This makes injective flows

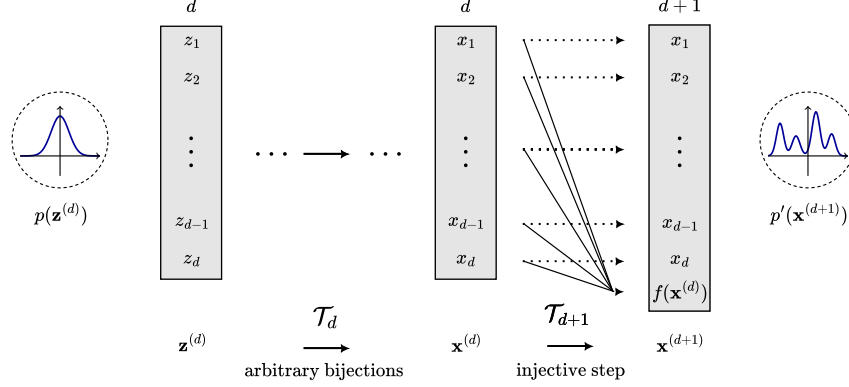


Figure 1: Architecture of proposed injective flows for parametric hypersurfaces, see Theorem 1

computationally prohibitive in high dimensional settings. We could make the injective transformation lightweight and stack expressive bijective layers before and after the injective step. However, the Jacobian determinant would still require cubic complexity. To see this, consider the transformation  $\mathcal{T} = \mathcal{T}_d \circ \mathcal{T}_{m \rightarrow d} \circ \mathcal{T}_m$ , where  $\mathcal{T}_m : \mathbb{R}^m \mapsto \mathbb{R}^m$  and  $\mathcal{T}_d : \mathbb{R}^d \mapsto \mathbb{R}^d$  are arbitrary bijections. The Jacobian determinant of  $\mathcal{T}$  factorizes as follows:

$$\det J_{\mathcal{T}} = \det J_{\mathcal{T}_m} \sqrt{\det \left( (J_{\mathcal{T}_d} J_{\mathcal{T}_{m \rightarrow d}})^T J_{\mathcal{T}_d} J_{\mathcal{T}_{m \rightarrow d}} \right)}. \quad (3)$$

We refer to Appendix A.1 for a full derivation. Note that we can factorize only  $\det J_{\mathcal{T}_m}$ , while the Jacobian determinant of the bijections  $\mathcal{T}_d$  after the injective step cannot be disentangled. We then need to compute the Jacobian product  $J_{\mathcal{T}_d} J_{\mathcal{T}_{m \rightarrow d}}$  and its determinant, which has cubic complexity.

### 3 Injective Flows for parametric hypersurfaces

We now present the two main results of the paper. Firstly, in Section 3.1 we propose injective flow to model densities on parametric hypersurfaces and we show how to compute the Jacobian determinant exactly and efficiently. Secondly, in Section 3.2 we consider the subset of star-like manifolds and extend the proposed injective flows to allow for a Cartesian representation of the density on the manifold. Also in this case the Jacobian determinant can be computed exactly and efficiently.

#### 3.1 Injective flows for parametric hypersurfaces

**Definition 1.** We define a *hypersurface*  $\mathcal{M}$  as a manifold of dimension  $d - 1$  embedded in  $\mathbb{R}^d$ . We call the hypersurface *parametric* if it allows a global parameterization, i.e. if there exists an injective function  $\varphi : z \in U \subset \mathbb{R}^{d-1} \mapsto \mathbb{R}^d$  such that any  $x \in \mathbb{R}^d$  on  $\mathcal{M}$  can be described as  $x = [z, \varphi(z)]^T$ .

**Proposed injective flows parametric hypersurfaces** We model the parametric hypersurface  $\mathcal{M}$  as  $\mathcal{T} = \mathcal{T}_{d+1} \circ \mathcal{T}_d$ .  $\mathcal{T}_d : \mathbb{R}^d \mapsto \mathbb{R}^d$  is an arbitrary bijection followed by an injective transformation  $\mathcal{T}_{d+1} : \mathbb{R}^d \mapsto \mathbb{R}^{d+1}$ , which inflates the dimensionality by one (see Figure 1). Since the inflation to the manifold happens as the last step of  $\mathcal{T}$ , the determinant of the combined transformation  $\mathcal{T}$  can be decomposed as  $\det J_{\mathcal{T}} = \det J_{\mathcal{T}_d} \det J_{\mathcal{T}_{d+1}}$  with  $\det J_{\mathcal{T}_{d+1}} = \sqrt{\det (J_{\mathcal{T}_{d+1}}^T J_{\mathcal{T}_{d+1}})}$  (see Eq. (3)). Crucially, explicitly computing  $\det J_{\mathcal{T}_{d+1}}$  would require  $O(d^3)$  complexity. Instead, in Theorem 1 we show how to compute  $\det J_{\mathcal{T}_{d+1}}$  analytically and efficiently in  $O(d)$ . We refer to Appendix A.3 for the full proof. Since the Jacobian determinant of standard bijections  $\det J_{\mathcal{T}_d}$  can be computed in  $O(d^2)$ , the overall complexity of the proposed injective flow is  $O(d^2)$ .

**Theorem 1.** Let  $\mathcal{T}_{d+1} : \mathbb{R}^d \mapsto \mathbb{R}^{d+1}$  be a transformation such that  $\mathcal{T}_{d+1} : x \mapsto [x, f(x)]^T$ , where  $f : \mathbb{R}^d \mapsto \mathbb{R}$  is any differentiable function (see Figure 1). Then,  $\mathcal{T}_{d+1}$  is injective and its Jacobian

determinant is equal to

$$\det J_{\mathcal{T}_{d+1}} = \sqrt{1 + \sum_{i=1}^d \left( \frac{\partial f}{\partial x_i} \right)^2}. \quad (4)$$

Relevantly, the Jacobian determinant can be computed efficiently in  $O(d)$ .

*Proof sketch.* The injectivity of  $\mathcal{T}_{d+1}$  can be easily seen by noting that  $\mathbf{x} \neq \mathbf{x}' \implies [\mathbf{x}, f(\mathbf{x})] \neq [\mathbf{x}', f(\mathbf{x}')] independently of  $f$ . We can then use the Jacobian determinant formula for injective transformations in Eq. (2). As a first step we consider the square matrix  $\tilde{J}_{\mathcal{T}_{d+1}} := [J_{\mathcal{T}_{d+1}}, \mathbf{0}_{d+1}] \in \mathbb{R}^{(d+1) \times (d+1)}$  and re-write the determinant in terms of the pseudo-determinant  $\text{Det}$  as$

$$\det J_{\mathcal{T}_{d+1}} = \sqrt{\det \left( J_{\mathcal{T}_{d+1}}^T J_{\mathcal{T}_{d+1}} \right)} = \sqrt{\text{Det} \left( \tilde{J}_{\mathcal{T}_{d+1}}^T \tilde{J}_{\mathcal{T}_{d+1}} \right)},$$

where the pseudo-determinant is defined as the product of all non-negative eigenvalues. The equality follows from the fact that  $\tilde{J}_{\mathcal{T}_{d+1}}$  and  $J_{\mathcal{T}_{d+1}}$  have the same spectrum up to zero eigenvalues, so the determinant and the pseudo-determinant coincide. The rest of the proof is based on the key observation that  $\tilde{J}_{\mathcal{T}_{d+1}}$  has rank  $d$  or, equivalently, that its null space is one-dimensional. Let the adjugate  $\text{adj } A$  of  $A \in \mathbb{R}^{(d+1) \times (d+1)}$  be defined as  $A \text{adj } A = \det A \mathbb{I}_{d+1}$ . One key property is that if  $\text{rank } A = \dim A - 1$ , then  $\text{Det } A = \text{Tr}(\text{adj } A)$  (Lemma 2). We can then rewrite the pseudo-determinant as

$$\text{Det} \left( \tilde{J}_{\mathcal{T}_{d+1}}^T \tilde{J}_{\mathcal{T}_{d+1}} \right) = \text{Tr} \left( \text{adj} \left( \tilde{J}_{\mathcal{T}_{d+1}}^T \tilde{J}_{\mathcal{T}_{d+1}} \right) \right) = \text{Tr} \left( \text{adj} \left( \tilde{J}_{\mathcal{T}_{d+1}} \right) \text{adj} \left( \tilde{J}_{\mathcal{T}_{d+1}}^T \right) \right),$$

where we used that  $\text{adj}(AB) = \text{adj}(B) \text{adj}(A)$  for any square matrices. Since  $\tilde{J}_{\mathcal{T}_{d+1}}$  has rank  $d$ , its right and left nullspaces are one dimensional. We can pick  $x \in \mathbb{R}^{d+1} \mid \tilde{J}_{\mathcal{T}_{d+1}} x = 0$  to span the right nullspace and  $y \in \mathbb{R}^{d+1} \mid \tilde{J}_{\mathcal{T}_{d+1}}^T y = 0$  to span the left nullspace. In such cases Lemma 1 holds:

$$\text{adj}(\tilde{J}_{\mathcal{T}_{d+1}}) = \frac{\text{Det}(\tilde{J}_{\mathcal{T}_{d+1}})}{y^T x} x y^T.$$

In our specific case  $y = [-\nabla f, 1]^T$  and  $x = [\mathbf{0}_d, 1]^T$  so we obtain

$$\text{Det} \left( \tilde{J}_{\mathcal{T}_{d+1}}^T \tilde{J}_{\mathcal{T}_{d+1}} \right) = \frac{\text{Det}(\tilde{J}_{\mathcal{T}_{d+1}})^2}{(y^T x)^2} \text{Tr} \left( (x y^T)^T x y^T \right) = y^T y = 1 + \sum_{i=1}^d \left( \frac{\partial f}{\partial x_i} \right)^2,$$

where we used that  $\text{Det}(\tilde{J}_{\mathcal{T}_{d+1}}) = 1$ ,  $y^T x = 1$  and  $x^T x = 1$ . ■

In variational inference settings we assume the manifold to be known. However, by making the injective transformation learnable we can extend the present framework to density estimation settings where the underlying manifold is unknown but assumed to be  $d - 1$  dimensional. As a side product, we would obtain an explicit parametrization of the manifold.

### 3.2 Injective flows for star-like manifolds

**Motivation** The injective flows introduced in Section 3.1 describe points on  $\mathcal{M}$  with the coordinate system induced by the parametrization  $\mathbf{x} = [\mathbf{z}, \varphi(\mathbf{z})]^T$ . If the target distribution (for variational inference) or the data-points (for density estimation) are expressed in such a coordinate system, the injective flows can be readily used. However, in some applications it is preferable to model the density with the usual Cartesian coordinates. We now consider a subclass of parametric hypersurfaces called star-like manifolds and extend the proposed framework to always allow for a Cartesian representation. We first define a star-like manifold and note that it can always be parameterized with generalized spherical coordinates. We then compose the injective flow with a spherical to Cartesian transformation. Relevantly, we show that the Jacobian determinant of the whole transformation can still be computed exactly and efficiently with the same time complexity of standard NFs.

**Definition 2.** We define the  $d$ -spherical coordinate system as a generalization of the spherical coordinate system for  $d$ -dimensional Euclidean spaces. Such coordinate system is defined with  $d - 1$  angles  $\theta_1, \dots, \theta_{d-1}$  and one radius  $r \in \mathbb{R}_{>0}$ , where  $\theta_i \in [0, \pi]$  for  $i < d - 1$  and  $\theta_{d-1} \in [0, 2\pi]$ . We further define a transformation  $\mathcal{T}_{s \rightarrow c} : \mathbf{x}_s \mapsto \mathbf{x}_c$  that maps spherical coordinates  $\mathbf{x}_s = [\theta_1, \dots, \theta_{d-1}, r]^T$  to Cartesian coordinates  $\mathbf{x}_c = [x_1, \dots, x_d]^T$  as

$$\begin{cases} x_1 = r \cos \theta_1 \\ x_2 = r \sin \theta_1 \cos \theta_2 \\ \vdots \\ x_{d-1} = r \sin \theta_1 \sin \theta_2 \cdots \sin \theta_{d-2} \cos \theta_{d-1} \\ x_d = r \sin \theta_1 \sin \theta_2 \cdots \sin \theta_{d-2} \sin \theta_{d-1} \end{cases} \quad (5)$$

In the following we denote with  $U_\theta^{d-1} \times \mathbb{R}_{>0}$  the domain of definition for  $d$ -spherical coordinate system, where  $U_\theta^{d-1} := [0, \pi]^{d-2} \times [0, 2\pi]$ .

**Definition 3.** We call a domain a *star domain*  $\mathcal{S}$  if there exist one point  $s_0 \in \mathcal{S}$  such that, given any other point  $s \in \mathcal{S}$  in the domain, the line segment connecting  $s_0$  to  $s$  lies entirely in  $\mathcal{S}$ . Furthermore, we define *star-like manifold*  $\mathcal{M}_\mathcal{S}$  as the manifold defined by the boundary of a star domain.

**Parameterization of star-like manifolds in spherical coordinates** Let  $\mathcal{M}_\mathcal{S}$  be a  $d - 1$  dimensional star-like manifold embedded in  $\mathbb{R}^d$ . Then, we need  $d - 1$  variables to identify any point  $\mathbf{x} \in \mathcal{M}_\mathcal{S}$ . In particular, we can parametrize  $\mathbf{x} = [\boldsymbol{\theta}, r(\boldsymbol{\theta})]^T$  with  $d - 1$  spherical angles  $\boldsymbol{\theta} \in U_\theta^{d-1}$  and a suitable radius function  $r(\boldsymbol{\theta})$ . If we choose  $s_0$  as the origin of the spherical coordinate system, we can define the radius as the line segment connecting  $\mathbf{x}$  and  $s_0$ . Crucially, by definition of star-like manifolds, the segment intersects the manifold only once, so the radius is uniquely defined. See Figure 2 for a graphical representation. Star-like manifolds are the most general class of manifolds that always allow such parameterization.

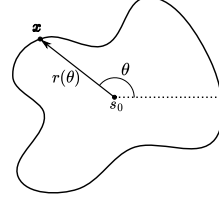


Figure 2: 2D star-like manifold parameterized in spherical coordinates.

**Proposed injective flows for star-like manifolds** We now exploit the spherical parametrization of star-like manifolds to define an injective flow where the density is expressed in Cartesian coordinates. The injective flow consists of three transformations  $\mathcal{T} := \mathcal{T}_{s \rightarrow c} \circ \mathcal{T}_r \circ \mathcal{T}_\theta$  (see Figure 3): (i) an arbitrary diffeomorphism to  $d$ -spherical angles  $\mathcal{T}_\theta : \mathbb{R}^{d-1} \mapsto U_\theta^{d-1}$ , (ii) the injective transformation that parameterizes the radius as a function of the angles  $\mathcal{T}_r : \mathbb{R}^{d-1} \mapsto \mathbb{R}^d$  and (iii) the  $d$ -spherical to Cartesian transformation  $\mathcal{T}_{s \rightarrow c} : \mathbb{R}^d \mapsto \mathbb{R}^d$ . In practice, we can increase the flexibility of  $\mathcal{T}_\theta$  by stacking any bijective layers of choice, as shown in Figure 3. In Theorem 2 we show that the Jacobian determinant of the full transformation can be computed analytically and efficiently in  $O(d^2)$ .

**Theorem 2.** Let  $\mathcal{T} := \mathcal{T}_{s \rightarrow c} \circ \mathcal{T}_r \circ \mathcal{T}_\theta$  as in Figure 3, where  $\mathcal{T}_\theta : \mathbf{z} \in \mathbb{R}^{d-1} \mapsto \boldsymbol{\theta} \in U_\theta^{d-1}$  is any diffeomorphism to  $d$ -spherical angles,  $\mathcal{T}_r : \boldsymbol{\theta} \in U_\theta^{d-1} \mapsto [\boldsymbol{\theta}, r(\boldsymbol{\theta})] \in U_\theta^{d-1} \times \mathbb{R}_{>0}$  a transformation as in Theorem 1 with  $r : \boldsymbol{\theta} \in U_\theta^{d-1} \mapsto r \in \mathbb{R}_{>0}$  being differentiable, and  $\mathcal{T}_{s \rightarrow c} : [\boldsymbol{\theta}, r(\boldsymbol{\theta})]^T \in U_\theta^{d-1} \times \mathbb{R}_{>0} \mapsto \mathbf{x} \in \mathbb{R}^d$  the  $d$ -spherical to Cartesian transformation as in Definition 2.

Then, the Jacobian determinant of the full transformation  $\mathcal{T}$  is equal to

$$\det J_\mathcal{T} = \det J_{\mathcal{T}_\theta} \det J_{\mathcal{T}_{s \rightarrow c}} \|(J_{\mathcal{T}_{s \rightarrow c}}^T)^{-1} \mathbf{y}\|_F, \quad (6)$$

where  $\mathbf{y} := [-\nabla_{\boldsymbol{\theta}} r(\boldsymbol{\theta}), 1]^T$  and  $\|\cdot\|_F$  is the Frobenius norm. Relevantly, the Jacobian determinant in Eq. (6) can still be computed efficiently in quadratic time.

*Proof sketch.* The proof is similar in nature to that of Theorem 1, except that the calculations now involve the Jacobian of  $\mathcal{T}_{s \rightarrow c}$  as well. We show that can factor out  $\det J_{\mathcal{T}_{s \rightarrow c}}$  and that we are then only left with the linear system  $(J_{\mathcal{T}_{s \rightarrow c}}^T)^{-1} \mathbf{y}$  in Eq. (6). Naively solving the system would require  $O(d^3)$  complexity. Crucially, the matrix  $J_{\mathcal{T}_{s \rightarrow c}}^T$  is nearly triangular so we can make the system

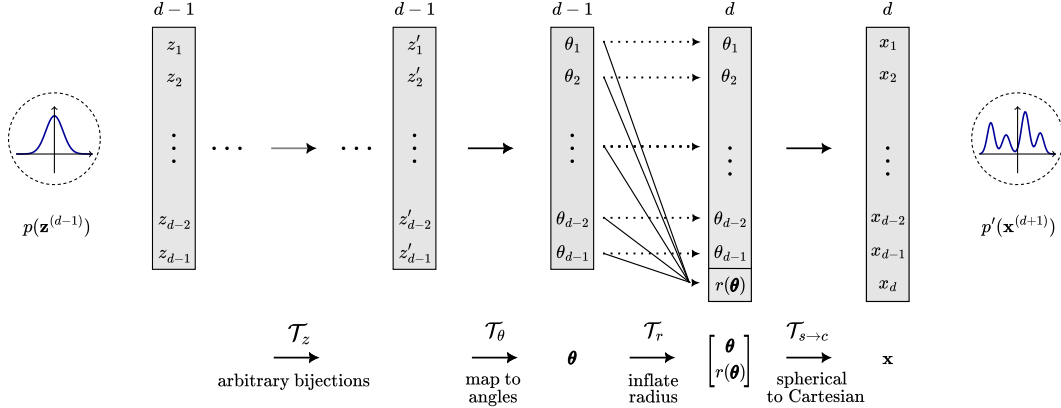


Figure 3: Architecture of the proposed injective flows for star-like manifolds, see Theorem 2.

triangular with one step of Gaussian elimination or, equivalently, we can compute the inverse with the Sherman–Morrison formula. In both cases we can solve the resulting triangular system in  $O(d^2)$ . Since  $\det(J_{\mathcal{T}_{s \rightarrow c}})^2$  is known analytically (see Eq.(28)) and  $\det J_{\mathcal{T}_\theta}$  is the usual Jacobian determinant for bijections, the Jacobian determinant of  $\mathcal{T}$  can be computed efficiently in  $O(d^2)$ . ■

### 3.3 Limitations

The main limitation of the proposed injective flows is that they provide exact and efficient Jacobian determinant for parametric hypersurfaces only. As we showcase, this class of manifolds is very relevant for variational inference applications. However, in density estimation tasks the data is often assumed to be generated from a much lower dimensional manifold. The present framework could be used when the manifold is assumed to be  $d - 1$  dimensional. As a side product, we would learn an explicit parametrization of the learnt manifold as well. Lastly, the expressive power of the proposed injective flows depends on the flexibility of the bijective layers. Despite state-of-the-art bijective layers being extremely expressive [Perugachi-Diaz et al., 2021], Liao and He [2021] showed that the number of modes that can be modeled is still limited.

## 4 Related work

**Normalizing Flows** Normalizing Flows (NFs) consist of a simple base distribution that is transformed into a more complicated one through a series of bijective transformations. One can show that such a construction allows to approximate any well-behaved distribution Papamakarios et al. [2021]. In practice, the bijective transformation are implemented with neural networks that show a trade-off between expressiveness and computational complexity. However, recently developed bijective layers provide very efficient transformations that satisfy the universality property [Huang et al., 2018, Durkan et al., 2019, Jaini et al., 2019]. For a comprehensive review of the different bijective layers and for an extensive discussion about application of NFs we refer to Papamakarios et al. [2021] and Kobyzev et al. [2021].

**Variational Inference with NFs** Due to the high expressive power and flexibility, NFs have become popular in two scenarios. Given some observations, NFs are used as generative models to first approximate the data generating distribution and to later sample new instances [Dinh et al., 2017, Papamakarios et al., 2017]. In variational inference settings, NFs are used to approximate a given unnormalized target distribution. Once trained, NFs allow to evaluate the (approximate) normalized distribution and to draw samples from it [Rezende and Mohamed, 2015, Kingma et al., 2016]. This setting is particularly useful in Bayesian inference [Louizos and Welling, 2017], where the goal is to learn and sample from the posterior distribution given the (unnormalized) product of the prior and likelihood. NFs have proven to be an attractive alternative to MCMC samplers [Negri et al., 2023]. In this work we focus on Bayesian variational inference.

**Injective Flows on manifolds** The computational bottleneck of injective flows is the evaluation of Jacobian determinant term in Eq. (2). For some trivial manifolds like  $d$ -dimensional spheres and tori, the Jacobian can be computed analytically [Gemici et al., 2016, Rezende et al., 2020]. However, this is not the case for most applications. Some early work proposed to separately learn the manifold and then learn the density on it, avoiding the computation of Jacobian determinant [Brehmer and Cranmer, 2020]. Unsurprisingly, Caterini et al. [2021] showed that this can have detrimental effects already in simple low-dimensional settings. Therefore, most work on normalizing flows for manifolds is focused on finding some tractable approximation to the Jacobian determinant. The most common one is to employ the Hutchinson’s trace estimator [Mathieu and Nickel, 2020, Caterini et al., 2021, Flouris and Konukoglu, 2023], which is characterized by high variance and it is actually biased if used to estimate the log-determinant of the Jacobian [Kumar et al., 2020]. State-of-the-art work employs surrogate log-likelihood loss and still approximate the Jacobian determinant [Sorrenson et al., 2024].

In contrast, we are the first to propose exact and computationally efficient injective flows for a wide class of manifolds, namely parametric hypersurfaces.

## 5 Applications

We showcase the relevance of the proposed approach in two applications. In Section 5.1 we use injective flows to define a novel Objective Bayes approach to penalized likelihood problems. In Section 5.2 we introduce a general framework for variational inference in Bayesian mixture models, where we constrain the posterior on the mixture weights on the probabilistic simplex by construction.

### 5.1 Objective Bayesian approach to penalized likelihood

**Objective and subjective Bayes** Bayesian inference is a powerful statistical method that requires a likelihood term, which explains the observed data, and a prior, which quantifies our initial belief. However, in many cases we might not have enough problem-specific knowledge to specify an informative subjective prior. This led to the development of *objective priors*, which are designed to be minimally informative. Some objective priors include Jeffreys rule [Jeffreys, 1961], reference priors [Bernardo, 1979], and maximum entropy priors [Jaynes, 2003]. Given the vast literature on objective priors [Berger, 2006], in this work we do not intend to discuss if objective priors should be preferable. Instead, we provide a new framework to define objective priors in settings where only subjective ones have been explored so far. One such setting is penalized likelihood problems.

**Objective Bayes for penalized likelihood models** Penalized likelihood methods are very popular approaches for variable selection in high-dimensional settings. We assume a normal linear regression model:  $\mathbf{y} \sim \mathbf{X}\boldsymbol{\beta} + \boldsymbol{\epsilon}$  with  $\boldsymbol{\epsilon} \sim \mathcal{N}(\mathbf{0}, \sigma^2 \mathbb{I}_n)$ , where  $\mathbf{X} \in \mathbb{R}^{n \times d}$  is the data matrix,  $\mathbf{y} \in \mathbb{R}^n$  the targets and  $\boldsymbol{\beta} \in \mathbb{R}^d$  the regression coefficients. We then optimize the mean-squared error  $\|\mathbf{y} - \mathbf{X}\boldsymbol{\beta}\|_2^2$  subject to the (pseudo-) norm penalties  $\|\boldsymbol{\beta}\|_p^p$  with  $p > 0$ , which encourages sparsity for  $p \leq 1$ . The framework can be easily extended to more general penalties. Note that for  $p = 1$  we recover the LASSO penalty [Tibshirani, 1996] and for  $p = 2$  the Ridge penalty. Tibshirani [1996] noted that we can interpret such penalized likelihood in a Bayesian way by specifying a Gaussian likelihood and a suitable prior. Park and Casella [2008] showed that with an independent Laplace prior the Maximum a Posterior (MAP) estimate of the posterior coincides with the frequentist solution. The above reasoning can be extended to any  $l_p$  (pseudo-) norm  $\|\cdot\|_p$  by using the generalized Gaussian distribution as prior  $p(\boldsymbol{\beta}|\lambda) \propto \prod_i \exp\{-\lambda|\beta_i|^p\}$ :

$$\arg \min_{\boldsymbol{\beta} \in \mathbb{R}^d} \frac{1}{2\sigma^2} \|\mathbf{y} - \mathbf{X}\boldsymbol{\beta}\|_2^2 + \lambda \|\boldsymbol{\beta}\|_p^p = \arg \max_{\boldsymbol{\beta} \in \mathbb{R}^d} \underbrace{\mathcal{N}(\mathbf{X}\boldsymbol{\beta}, \sigma^2 \mathbb{I}_n)}_{p(\mathbf{y}|\mathbf{X}, \boldsymbol{\beta})} \underbrace{\prod_i \exp\{-\lambda|\beta_i|^p\}}_{p(\boldsymbol{\beta}|\lambda)} = \boldsymbol{\beta}^* . \quad (7)$$

However, the generalized Gaussian is not the only prior for which Eq. (7) holds. Any monotonic transformation  $h$  of  $p(\boldsymbol{\beta}|\lambda)$  results in the same contour lines of the penalty and hence in the same MAP solution  $\boldsymbol{\beta}^*$  (for an appropriately rescaled  $\lambda$ ). Therefore, the choice of  $h(p(\boldsymbol{\beta}|\lambda))$  is subjective but, crucially, it influences the posterior distribution. We show this empirically on toy data by considering the Laplace prior and two simple monotonic transformations: its square (“square laplace”) and its square root (“root laplace”). In Figure 4 we can clearly see how the monotonic transformation influences the posterior. We provide more details in Appendix A.6, where we

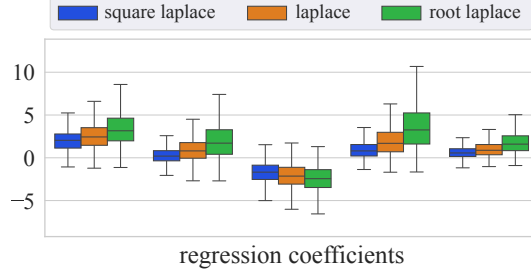


Figure 4: 95% posterior C.I. for monotonically transformed subjective priors.

also show that the Laplace prior and its monotonic transformation converge to the same MAP (see Figure 7). In contrast, we circumvent the choice of a subjective prior and propose a general framework for designing objective priors for penalized likelihood methods.

**Objective Bayesian penalized likelihood with injective flows** All choices of subjective priors in Eq. (7) enforce in the MAP limit the penalty  $\|\beta\|_p^p$  as a soft constraint controlled by  $\lambda$  such that  $\|\beta\|_p \leq k(\lambda)$ . Our idea is to enforce the norm penalty as a hard constraint by defining the posterior on the manifold  $\|\beta\|_p = k$  by construction. This way we do not require to *explicitly* specify a subjective prior and we are *implicitly* assuming a uniform prior on the manifold  $\|\beta\|_p = k$ , which otherwise would be very challenging to explicitly derive. We summarize the two approaches below:

<p><i>Objective Bayes</i></p> $p(\mathbf{y} \mathbf{X}, \beta) = \mathcal{N}(\mathbf{X}\beta, \sigma^2\mathbb{I}_n)$ <p>posterior on manifold: <math>\ \beta\ _p = k</math></p>	$\longleftrightarrow$	<p><i>Subjective Bayes</i></p> $p(\mathbf{y} \mathbf{X}, \beta) = \mathcal{N}(\mathbf{X}\beta, \sigma^2\mathbb{I}_n)$ <p>prior: <math>p(\beta \lambda) \propto \prod_i \exp\{-\lambda \beta_i ^p\}</math></p>
---	-----------------------	---

On top of resolving the ambiguity arising from the subjective choice of the prior, the proposed objective prior is particularly useful for expressing the solution path directly as a function of the norm  $\|\beta\|_p$ , which is common practice in the literature [Park and Casella, 2008]. The equality  $\|\beta\|_p = k$  induces a star-like manifold which we can parametrize with a suitable radius function (see Eq. (34) for the explicit parametrization). Therefore, with the proposed framework we can define the (approximate) posterior  $q_\theta(\beta)$  to be constrained on  $\|\beta\|_p = k$  by construction.

We now illustrate the differences between the subjective and objective approaches with synthetic data. We use a NF to approximate the posterior  $\mathcal{N}(\mathbf{X}\beta\sigma^2\mathbb{I}_n)p(\beta|\lambda)$  with the “square laplace” subjective prior  $p(\beta|\lambda)$ . We choose  $\lambda$  such that the MAP has a specific norm  $\|\beta^*\|_1 = k$ . Further, we use an injective flow defined on  $\|\beta\|_1 = k$  to approximate the posterior given by the likelihood  $\mathcal{N}(\mathbf{X}\beta, \sigma^2\mathbb{I}_n)$ . In both cases training is performed by minimizing the reverse KL divergence. Figure 5 shows a fundamental difference between the two models: samples from the objective posterior lie exactly on the manifold while the subjective posterior is scattered out. The bottom panel of Figure 5 shows the distribution of the sample norms varying significantly with the choice of the subjective prior, which agrees with the findings in Figure 4. We include more implementation details in Appendix A.6.

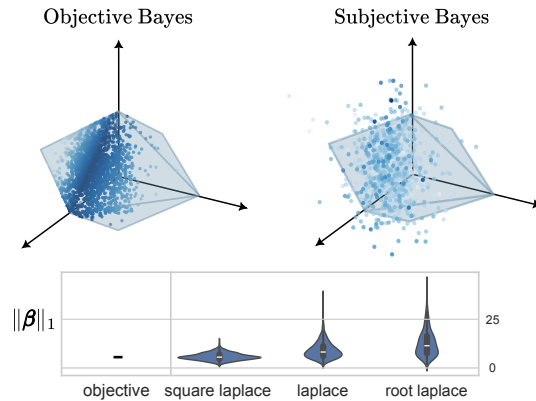


Figure 5: Comparison of objective and subjective Bayes in terms of posterior samples and their norm.

## 5.2 Variational Inference on Bayesian mixture models

**Bayesian mixture models** With mixture models we denote a general class of methods that rely on the concept of mixture components  $\pi$ , which are defined on the probabilistic simplex  $\mathcal{C}^d :=$



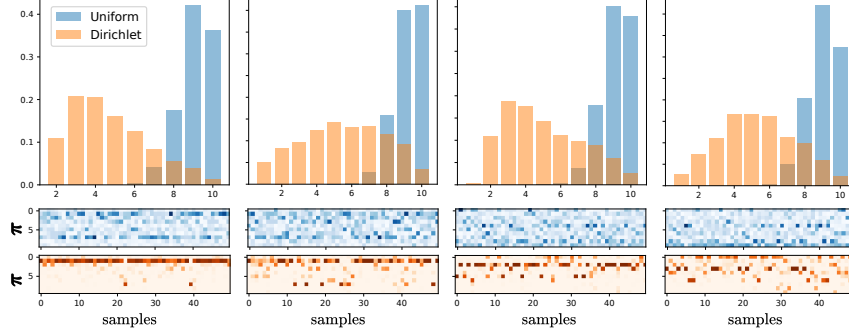


Figure 6: Number of non-zero entries in posterior samples for 4 fixed likelihood values. We compare uniform with Dirichlet prior, which encourages sparsity in the mixture weights  $\pi$ .

$\{\pi \in \mathbb{R}^d : \pi_i \geq 0, \sum_{i=1}^k \pi_i = 1\}$ . In the most general Bayesian formulation, we require a prior  $p(\pi)$  and some likelihood  $p(\mathcal{D}|\pi)$  to explain the observations  $\mathcal{D}$ . The challenge is then to define the posterior  $p(\pi|\mathcal{D}) \propto p(\mathcal{D}|\pi)p(\pi)$  on the probabilistic simplex  $\mathcal{C}^d$ . Most approaches rely on the Dirichlet distribution, which is defined on  $\mathcal{C}^d$  by construction:  $\text{Dir}(\pi) \propto \prod_i \pi_i^{\alpha_i - 1}$  with  $\alpha_i > 0$ . With a Dirichlet prior and a multinomial likelihood, the posterior is also a Dirichlet distribution, hence defined on  $\mathcal{C}^d$ . As a more flexible alternative to MCMC methods, we present a general variational inference framework where  $p(\pi|\mathcal{D})$  is always defined on  $\mathcal{C}^d$ , leaving complete freedom in the choice of prior and likelihood. Notably, defining a variational family on a manifold is not trivial in general.

**Injective flows for posterior inference in Bayesian mixture model** The probabilistic simplex  $\mathcal{C}^d$  is a star-like manifold, since it is equal to the  $l_1$  norm ball restricted to the positive quadrant; see Eq. (35) for the explicit parametrization. Therefore, with the proposed framework we can define an injective flow  $q_\theta(\pi)$  on  $\mathcal{C}^d$  by construction and train it to approximate the posterior  $p(\pi|\mathcal{D}) \propto p(\mathcal{D}|\pi)p(\pi)$ . In its most simple formulation, if no prior is specified, we are implicitly assuming a uniform distribution on the simplex, which is equivalent to a Dirichlet prior with  $\alpha_i = 1 \forall i$ . In the more general case, we can easily specify any combination of likelihood  $p(\mathcal{D}|\pi)$  and prior  $p(\pi)$ , and the (approximate) posterior  $q_\theta(\pi)$  will always be defined on  $\mathcal{C}^d$  by construction.

**Application: Uncertainty quantification in Bayesian portfolio optimization** For simplicity, we select a minimal example of Bayesian mixture model (according to the above definition) where conjugate distributions are not applicable. One such setting is index replication in the context of portfolio optimization [Markowitz and Todd, 2000]. A portfolio is defined as a set of  $n$  stocks which are held proportionally to the mixture components  $\pi \in \mathbb{R}_{>0}^n$ , such that  $\sum_i \pi_i = 1$ . Let  $\mathbf{R} \in \mathbb{R}^{T \times n}$  be the returns over the time-steps  $t = \{1, \dots, T\}$  of the  $n$  stocks. We are interested in optimizing the portfolio weights  $\pi$  such that we replicate the reference index returns  $\rho \in \mathbb{R}^T$ , while also incorporating investors personal preferences. For instance, a sparse portfolio allows to reduce transactions costs arising from trading [Sokolov and Polson, 2019]. We formulate the above problem in Bayesian fashion by specifying a Gaussian likelihood  $p(\rho|\mathbf{R}, \pi) = \mathcal{N}(\mathbf{R}\pi, \sigma^2 \mathbb{I}_n)$  and some sparsity-inducing prior  $p(\pi)$ .

With the proposed framework we can approximate the posterior  $p(\pi|\mathbf{R}, \rho) \propto p(\rho|\mathbf{R}, \pi)p(\pi)$  with an injective flow  $q_\theta(\pi)$  defined on  $\mathcal{C}^n$  by design. The flow  $q_\theta(\pi)$  is trained by minimizing the reverse K1 divergence with the unnormalized target  $p(\rho|\mathbf{R}, \pi)p(\pi)$ . For the sake of illustration, we select a portfolio with 10 stocks over a period of 200 time steps from the dataset in Xueyong Tu [2024]. We define  $q_\theta(\pi)$  on the manifold and consider two priors: the uniform prior on the simplex and the Dirichlet distribution. In Figure 6 we show the distribution of non-zero entries of the posterior samples for the uniform and Dirichlet distribution. In particular, we consider the distribution and the sparsity patterns at 4 fixed values of the likelihood (one per plot). Despite the likelihood being the same, the Dirichlet prior leads to a sparser solution with fewer non-zero entries. This is also noticeable in the sparsity patterns of the posterior samples in the bottom panel. In Appendix A.6 in Figure 9 we also show the cumulative return and how it is affected by sparsity. Overall, we showed how easily we can specify any likelihood and priors while constraining the posterior on the simplex.

## 6 Conclusions

Current work on injective flows on manifolds rely on approximations or lower bounds to circumvent the computation of the Jacobian determinant term. In this work we showed how to exactly and efficiently compute the Jacobian determinant term for a class of manifolds termed parametric hypersurfaces. For the subclass of star-like manifolds, we further provided an efficient way to get a Cartesian representation of the density on the manifold.

We also highlighted the importance of modeling densities on star-like manifolds in the context of variational inference. First, with the proposed framework we introduced a novel Objective Bayes approach to penalized likelihood methods. The idea is to circumvent the choice of a subjective prior by constraining the posterior on the manifold defined by level-sets of the prior. Second, we introduced a general variational inference framework for modeling the posterior over the mixture weights in Bayesian Mixture models. Overall, the proposed framework allows to efficiently model distributions on arbitrary parametric hypersurfaces and to flexibly specify any choice of prior and likelihood.

## References

- Lawrence Cayton. Algorithms for manifold learning. eScholarship, University of California, 2005.
- Mevlana C. Gemici, Danilo Rezende, and Shakir Mohamed. Normalizing flows on riemannian manifolds, 2016.
- Danilo Jimenez Rezende, George Papamakarios, Sebastien Racaniere, Michael Albergo, Gurtej Kanwar, Phiala Shanahan, and Kyle Cranmer. Normalizing flows on tori and spheres. In *Proceedings of the 37th International Conference on Machine Learning*. PMLR, 2020.
- Abhishek Kumar, Ben Poole, and Kevin Murphy. Regularized autoencoders via relaxed injective probability flow. In *Proceedings of the Twenty Third International Conference on Artificial Intelligence and Statistics*. PMLR, 2020.
- Anthony L. Caterini, Gabriel Loaiza-Ganem, Geoff Pleiss, and John Patrick Cunningham. Rectangular flows for manifold learning. In *Advances in Neural Information Processing Systems*, 2021.
- Peter Sorrenson, Felix Draxler, Armand Rousselot, Sander Hummerich, Lea Zimmermann, and Ullrich Koethe. Lifting architectural constraints of injective flows. In *The Twelfth International Conference on Learning Representations*, 2024.
- W. Rudin. *Real and Complex Analysis*. Mathematics series. McGraw-Hill, 1987. ISBN 9780071002769.
- Steven G Krantz and Harold R Parks. *Geometric integration theory*. Springer Science & Business Media, 2008.
- Yura Perugachi-Diaz, Jakub Tomczak, and Sandjai Bhulai. Invertible densenets with concatenated lipswish. In *Advances in Neural Information Processing Systems*. Curran Associates, Inc., 2021.
- Huadong Liao and Jiawei He. Jacobian determinant of normalizing flows, 2021.
- George Papamakarios, Eric Nalisnick, Danilo Jimenez Rezende, Shakir Mohamed, and Balaji Lakshminarayanan. Normalizing flows for probabilistic modeling and inference. *Journal of Machine Learning Research*, 22(57):1–64, 2021.
- Chin-Wei Huang, David Krueger, Alexandre Lacoste, and Aaron Courville. Neural autoregressive flows. In *Proceedings of the 35th International Conference on Machine Learning*, volume 80 of *Proceedings of Machine Learning Research*, pages 2078–2087. PMLR, 10–15 Jul 2018.
- Conor Durkan, Artur Bekasov, Iain Murray, and George Papamakarios. Neural spline flows. In *Advances in Neural Information Processing Systems*, volume 32. Curran Associates, Inc., 2019.
- Priyank Jaini, Kira A. Selby, and Yaoliang Yu. Sum-of-squares polynomial flow. In *Proceedings of the 36th International Conference on Machine Learning*, volume 97 of *Proceedings of Machine Learning Research*, pages 3009–3018. PMLR, 09–15 Jun 2019.
- Ivan Kobyzev, Simon J.D. Prince, and Marcus A. Brubaker. Normalizing flows: An introduction and review of current methods. *IEEE Transactions on Pattern Analysis and Machine Intelligence*, 43(11):3964–3979, November 2021. ISSN 1939-3539.
- Laurent Dinh, Jascha Sohl-Dickstein, and Samy Bengio. Density estimation using real NVP. In *International Conference on Learning Representations*, 2017.
- George Papamakarios, Theo Pavlakou, and Iain Murray. Masked autoregressive flow for density estimation. In *Advances in Neural Information Processing Systems*, volume 30. Curran Associates, Inc., 2017.
- Danilo Rezende and Shakir Mohamed. Variational inference with normalizing flows. In *Proceedings of the 32nd International Conference on Machine Learning*, pages 1530–1538. PMLR, 2015.
- Durk P Kingma, Tim Salimans, Rafal Jozefowicz, Xi Chen, Ilya Sutskever, and Max Welling. Improved variational inference with inverse autoregressive flow. In *Advances in Neural Information Processing Systems*, 2016.

- Christos Louizos and Max Welling. Multiplicative normalizing flows for variational Bayesian neural networks. In *Proceedings of the 34th International Conference on Machine Learning*, Proceedings of Machine Learning Research, pages 2218–2227. PMLR, 06–11 Aug 2017.
- Marcello Massimo Negri, Fabricio Arend Torres, and Volker Roth. Conditional matrix flows for gaussian graphical models. In *Thirty-seventh Conference on Neural Information Processing Systems*, 2023.
- Johann Brehmer and Kyle Cranmer. Flows for simultaneous manifold learning and density estimation. In *Advances in Neural Information Processing Systems*, volume 33. Curran Associates, Inc., 2020.
- Emile Mathieu and Maximilian Nickel. Riemannian continuous normalizing flows. In *Advances in Neural Information Processing Systems*, volume 33. Curran Associates, Inc., 2020.
- Kyriakos Flouris and Ender Konukoglu. Canonical normalizing flows for manifold learning. In *Thirty-seventh Conference on Neural Information Processing Systems*, 2023.
- Harold Jeffreys. *The theory of probability*. Oxford University Press, 1961.
- Jose M Bernardo. Reference posterior distributions for bayesian inference. *Journal of the Royal Statistical Society Series B: Statistical Methodology*, 1979.
- Edwin T Jaynes. *Probability theory: The logic of science*. Cambridge university press, 2003.
- James Berger. The case for objective Bayesian analysis. *Bayesian Analysis*, 1(3), 2006.
- Robert Tibshirani. Regression shrinkage and selection via the lasso. *Journal of the Royal Statistical Society. Series B (Methodological)*, 58(1):267–288, 1996. ISSN 00359246.
- Trevor Park and George Casella. The bayesian lasso. *Journal of the american statistical association*, 103(482), 2008.
- Harry M Markowitz and G Peter Todd. *Mean-variance analysis in portfolio choice and capital markets*, volume 66. John Wiley & Sons, 2000.
- Vadim Sokolov and Michael Polson. Strategic bayesian asset allocation, 2019.
- Bin Li Xueyong Tu. “robust portfolio selection with smart return prediction”, 2024. data retrieved from Mendeley Data, 10.17632/gx66wsgwkr.1.
- Kenier Castillo and Ion Zaballa. On a formula of thompson and mcenteggert for the adjugate matrix. *Linear Algebra and its Applications*, 2022. ISSN 0024-3795.
- Oliver Knill. Cauchy–binet for pseudo-determinants. *Linear Algebra and its Applications*, 459: 522–547, 2014. ISSN 0024-3795.
- Angel Muleshkov and Tan Nguyen. Easy proof of the jacobian for the n-dimensional polar coordinates. *Pi Mu Epsilon Journal*, 14(4):269–273, 2016.
- Vincent Stimper, David Liu, Andrew Campbell, Vincent Berenz, Lukas Ryll, Bernhard Schölkopf, and José Miguel Hernández-Lobato. normflows: A pytorch package for normalizing flows. *Journal of Open Source Software*, 2023.
- Fabricio Arend Torres, Marcello Massimo Negri, Marco Inversi, Jonathan Aellen, and Volker Roth. Lagrangian flow networks for conservation laws. In *The Twelfth International Conference on Learning Representations*, 2024.
- Diederik P. Kingma and Jimmy Ba. Adam: A method for stochastic optimization, 2017.

## A Appendix

The Appendix is organized in six parts. In Subsection A.1 and A.2 we provide some auxiliary theorems and Lemmas that are used in the two main proofs. In Subsection A.3 and Subsection A.4 we provide the full proof of Theorem 1 and Theorem 2, respectively. In Subsection A.5 we provide some details about the implementation of the proposed injective flows and we make some further comments about the associated computational cost. Finally, in Subsection A.6 we include further plots and implementation details about the experiments.

### A.1 Jacobian determinant for arbitrary injective flows

**Remark 1.** Let  $\mathcal{T}_m : \mathbb{R}^m \mapsto \mathbb{R}^m$  and  $\mathcal{T}_d : \mathbb{R}^d \mapsto \mathbb{R}^d$  be arbitrary bijective transformation and let  $\mathcal{T}_{m \rightarrow d} : \mathbb{R}^m \rightarrow \mathbb{R}^d$  be an injective transformation. The transformation  $\mathcal{T} = \mathcal{T}_d \circ \mathcal{T}_{m \rightarrow d} \circ \mathcal{T}_m$  is also injective and its Jacobian determinant factorizes as

$$\det J_{\mathcal{T}} = \det J_{\mathcal{T}_m} \sqrt{\det \left( (J_{\mathcal{T}_d} J_{\mathcal{T}_{m \rightarrow d}})^T J_{\mathcal{T}_d} J_{\mathcal{T}_{m \rightarrow d}} \right)}. \quad (8)$$

*Proof.* The injectivity of  $\mathcal{T}$  is trivial since it is by definition a composition of injective functions. Since  $\mathcal{T}$  is injective, its Jacobian matrix  $J_{\mathcal{T}} \in \mathbb{R}^{d \times m}$  is not squared and we cannot use the usual property of bijections in Eq.(1). Instead, we use the definition of Jacobian determinant for injective functions in Eq. (2):

$$\det J_{\mathcal{T}} = \sqrt{\det \left( J_{\mathcal{T}}^T J_{\mathcal{T}} \right)} = \sqrt{\det \left( (J_{\mathcal{T}_d} J_{\mathcal{T}_{m \rightarrow d}} J_{\mathcal{T}_m})^T (J_{\mathcal{T}_d} J_{\mathcal{T}_{m \rightarrow d}} J_{\mathcal{T}_d}) \right)}, \quad (9)$$

where  $J_m \in \mathbb{R}^{m \times m}$ ,  $J_{\mathcal{T}_{m \rightarrow d}} \in \mathbb{R}^{d \times m}$  and  $J_{\mathcal{T}_d} \in \mathbb{R}^{d \times d}$ . We now show that we can factor out the Jacobian determinant of  $\mathcal{T}_m$ , i.e. the bijection that precedes the dimensional inflation step with  $\mathcal{T}_{m \rightarrow d}$ . To do so we use the property that for square matrices  $A, B$   $\det(AB) = \det A \det B$  and that  $\det A = \det A^T$ :

$$\begin{aligned} \det J_{\mathcal{T}} &= \sqrt{\det \left( J_{\mathcal{T}_m}^T J_{\mathcal{T}_{m \rightarrow d}}^T J_{\mathcal{T}_d}^T J_{\mathcal{T}_d} J_{\mathcal{T}_{m \rightarrow d}} J_{\mathcal{T}_m} \right)} \\ &= \sqrt{\det J_{\mathcal{T}_m}^T \det \left( J_{\mathcal{T}_{m \rightarrow d}}^T J_{\mathcal{T}_d}^T J_{\mathcal{T}_d} J_{\mathcal{T}_{m \rightarrow d}} \right) \det J_{\mathcal{T}_m}} \\ &= \det J_{\mathcal{T}_m} \sqrt{\det \left( (J_{\mathcal{T}_d} J_{\mathcal{T}_{m \rightarrow d}})^T (J_{\mathcal{T}_d} J_{\mathcal{T}_{m \rightarrow d}}) \right)} \\ &= \det J_{\mathcal{T}_m} \det J_{\mathcal{T}_d \circ \mathcal{T}_{m \rightarrow d}}. \end{aligned} \quad (10)$$

■

### A.2 Auxiliary theorems: adjugate matrix and pseudo-determinant

**Theorem 3.** [Castillo and Zaballa, 2022] Let  $A \in \mathbb{R}^{d \times d}$  and let  $\lambda \in \mathbb{R}$  be an eigenvalue of  $A$ . Let  $v, w \in \mathbb{R}^d$  be a right and a left eigenvector, respectively, of  $A$  for  $\lambda$ . Then

$$w^T v \operatorname{adj}(\lambda \mathbb{I}_d - A) = p'_A(\lambda) v w^T. \quad (11)$$

where  $p'_A(\lambda)$  is the derivative of the characteristic polynomial  $p_A(\lambda) = \det(\lambda \mathbb{I}_d - A)$ .

**Lemma 1.** Consider the special case where  $A \in \mathbb{R}^{d \times d}$  and  $\operatorname{rank} A = d - 1$  or, in other words, the nullspace of  $A$  is one dimensional. Then

$$\operatorname{adj}(A) = \frac{\operatorname{Det}(A)}{w^T v} v w^T, \quad (12)$$

where  $\operatorname{Det}$  is the pseudo-determinant.

*Proof.* Since  $\text{rank } A = d - 1$ , then there exists one zero eigenvalue. For  $\lambda = 0$  Theorem 3 reduces to  $w^T v \text{adj}(-A) = p'_A(0)vw^T$ . We can now use the following property of the adjugate matrix:  $\text{adj}(cA) = c^d \text{adj}(A)$  for any scalar  $c$ . As a particular case, for  $c = -1$  we have  $\text{adj}(-A) = (-)^d \text{adj}(A)$ . Therefore, we obtain that  $w^T v \text{adj}(A) = (-)^d p'_A(0)vw^T$ . Now, the pseudo-determinant is equal to the smallest non-zero coefficient of the characteristic polynomial  $p(\lambda) = \det(\lambda \mathbb{I}_d - A)$  [Knill, 2014]. If we expand the definition we obtain  $p(\lambda) = (-)^d p(A - \lambda \mathbb{I}) = p_0 \lambda^d + (-) p_1 \lambda^{d-1} + (-)^k p_k \lambda^{d-k} + (-)^d p_d$  (see Proposition 2, 8. in Knill [2014]). Since  $A$  has rank  $d - 1$ ,  $p_d = 0$  and the smallest non-zero coefficient is  $p_{d-1}$ . Finally, note that  $p'_A(0) = (-)^d p_{d-1} = (-)^d \text{Det}(A)$ . ■

**Lemma 2.** Consider the special case where  $A \in \mathbb{R}^{d \times d}$  and  $\text{rank } A = d - 1$ . Then,

$$\text{Tr}(\text{adj}(A)) = \text{Det}(A) . \quad (13)$$

*Proof.* We take the trace of the left and right-hand side of Eq. (12). We get  $\text{Tr}(\text{adj}(A)) = \frac{\text{Det}(A)}{w^T v} \text{Tr}(vw^T) = \frac{\text{Det}(A)}{w^T v} \text{Tr}(w^T v) = \text{Det}(A)$ . In the first equality we used the linearity of the trace and factored out the constants  $\text{Det}(A)$  and  $w^T v$ . Lastly, we used the cyclic property of the trace  $\text{Tr}(w^T v) = \text{Tr}(vw^T)$ . ■

### A.3 Proof of Theorem 1

**Theorem 1.** Let  $\mathcal{T}_{d+1} : \mathbb{R}^d \mapsto \mathbb{R}^{d+1}$  be a transformation such that  $\mathcal{T}_{d+1} : \mathbf{x} \mapsto [\mathbf{x}, f(\mathbf{x})]^T$ , where  $f : \mathbb{R}^d \mapsto \mathbb{R}$  is any differentiable function (see Figure 1). Then,  $\mathcal{T}_{d+1}$  is injective and its Jacobian determinant is equal to

$$\det J_{\mathcal{T}_{d+1}} = \sqrt{1 + \sum_{i=1}^d \left( \frac{\partial f}{\partial x_i} \right)^2} . \quad (4)$$

Relevantly, the Jacobian determinant can be computed efficiently in  $O(d)$ .

*Proof.* A transformation  $\mathcal{T}$  is injective if  $\forall \mathbf{x}, \mathbf{x}'$  in the domain, if  $\mathbf{x} \neq \mathbf{x}' \implies \mathcal{T}(\mathbf{x}) \neq \mathcal{T}(\mathbf{x}')$ . For  $\mathcal{T}_{d+1}$  this is apparent since  $\forall \mathbf{x}, \mathbf{x}'$ , if  $\mathbf{x} \neq \mathbf{x}'$  then clearly  $[\mathbf{x}, f(\mathbf{x})]^T \neq [\mathbf{x}', f(\mathbf{x}')]^T$ . As a first step we consider the square matrix  $\tilde{J}_{\mathcal{T}_{d+1}} := [J_{\mathcal{T}_{d+1}}, \mathbf{0}_{d+1}] \in \mathbb{R}^{d+1 \times d+1}$  and re-write the determinant in terms of the pseudo-determinant  $\text{Det}$  as

$$\det J_{\mathcal{T}_{d+1}} = \sqrt{\det \left( J_{\mathcal{T}_{d+1}}^T J_{\mathcal{T}_{d+1}} \right)} = \sqrt{\text{Det} \left( \tilde{J}_{\mathcal{T}_{d+1}}^T \tilde{J}_{\mathcal{T}_{d+1}} \right)} , \quad (14)$$

where the pseudo-determinant is defined as the product of all non-zero eigenvalues. In the first equality we used the definition of Jacobian determinant for injective transformations in Eq. 2. The second equality follows from the fact that  $J_{\mathcal{T}_{d+1}}^T J_{\mathcal{T}_{d+1}}$  and  $\tilde{J}_{\mathcal{T}_{d+1}}^T \tilde{J}_{\mathcal{T}_{d+1}}$  have the same spectrum up to zero eigenvalues, so the determinant of the former coincides with the pseudo-determinant of the latter (by definition). To see that they share the same spectrum up to one zero eigenvalue, consider the explicit structure of the matrix product:

$$\tilde{J}_{\mathcal{T}_{d+1}}^T \tilde{J}_{\mathcal{T}_{d+1}} = \begin{bmatrix} J_{\mathcal{T}_{d+1}}^T J_{\mathcal{T}_{d+1}} & \mathbf{0}_{d \times 1} \\ \mathbf{0}_{1 \times d} & 0 \end{bmatrix} . \quad (15)$$

The rest of the proof is based on the key observation that  $\tilde{J}_{\mathcal{T}_{d+1}}$  has rank  $d$  or, equivalently, that its null space is one-dimensional. Let the adjugate matrix  $\text{adj } A$  of  $A \in \mathbb{R}^{d+1 \times d+1}$  be defined as  $A \text{adj } A = \det A \mathbb{I}_{d+1}$ . Since  $\text{rank } A = \dim A - 1$ , we can use Lemma 2:  $\text{Det } A = \text{Tr}(\text{adj } A)$ . We can then rewrite the pseudo-determinant as

$$\text{Det} \left( \tilde{J}_{\mathcal{T}_{d+1}}^T \tilde{J}_{\mathcal{T}_{d+1}} \right) = \text{Tr} \left( \text{adj} \left( \tilde{J}_{\mathcal{T}_{d+1}}^T \tilde{J}_{\mathcal{T}_{d+1}} \right) \right) = \text{Tr} \left( \text{adj} \left( \tilde{J}_{\mathcal{T}_{d+1}} \right) \text{adj} \left( \tilde{J}_{\mathcal{T}_{d+1}}^T \right) \right) , \quad (16)$$

where we used that  $\text{adj}(AB) = \text{adj}(B) \text{adj}(A)$  for any square matrices  $A, B$ . Since  $\tilde{J}_{\mathcal{T}_{d+1}}$  has rank  $d$ , its nullspace is one dimensional and we can pick  $x \in \mathbb{R}^{d+1} \mid \tilde{J}_{\mathcal{T}_{d+1}} x = 0$  to span the entire

nullspace. The same holds true for  $\tilde{J}_{\mathcal{T}_{d+1}}^T$ , or equivalently for the left nullspace of  $J_{\mathcal{T}_{d+1}}$ , and we can pick  $y \in \mathbb{R}^{d+1} \mid \tilde{J}_{\mathcal{T}_{d+1}}^T y = 0$ . We can easily compute  $x$  and  $y$  by looking at the structure of  $\tilde{J}_{\mathcal{T}_{d+1}}$ :

$$\tilde{J}_{\mathcal{T}_{d+1}} = \begin{bmatrix} 1 & 0 & \cdots & 0 & 0 \\ 0 & 1 & & & 0 \\ \vdots & & \ddots & & \vdots \\ 0 & & & 1 & 0 \\ \frac{\partial f}{\partial x_1} & \frac{\partial f}{\partial x_2} & \cdots & \frac{\partial f}{\partial x_d} & 0 \end{bmatrix} \quad x := \begin{bmatrix} 0 \\ 0 \\ \vdots \\ 0 \\ 1 \end{bmatrix} \quad y := \begin{bmatrix} 0 \\ -\frac{\partial f}{\partial x_1} \\ -\frac{\partial f}{\partial x_2} \\ \vdots \\ -\frac{\partial f}{\partial x_d} \\ 1 \end{bmatrix}. \quad (17)$$

We now make use of Lemma 1 for  $\tilde{J}_{\mathcal{T}_{d+1}}$ , which gives us

$$\text{adj}(\tilde{J}_{\mathcal{T}_{d+1}}) = \frac{\text{Det}(\tilde{J}_{\mathcal{T}_{d+1}})}{y^T x} xy^T. \quad (18)$$

Note that  $y^T x$  is a scalar and  $xy^T \in \mathbb{R}^{d \times d}$  is a matrix. We can now substitute Eq. (18) in Eq. (16):

$$\text{Det}(\tilde{J}_{\mathcal{T}_{d+1}}^T \tilde{J}_{\mathcal{T}_{d+1}}) = \frac{\text{Det}(\tilde{J}_{\mathcal{T}_{d+1}})^2}{(y^T x)^2} \text{Tr}(xy^T (xy^T)^T) = y^T y = 1 + \sum_{i=1}^d \left( \frac{\partial f}{\partial x_i} \right)^2. \quad (19)$$

In the first equality we used that  $\text{adj}(A^T) = \text{adj}(A)^T$  and, since the trace is a linear operator, we took out  $\text{Det}(\tilde{J}_{\mathcal{T}_{d+1}})^2$  and  $(y^T x)^2$ . Lastly, in the second equality we substituted the numerical values  $\text{Det}(\tilde{J}_{\mathcal{T}_{d+1}}) = 1$ ,  $y^T x = 1$  and  $x^T x = 1$ . ■

#### A.4 Proof of Theorem 2

**Theorem 2.** Let  $\mathcal{T} := \mathcal{T}_{s \rightarrow c} \circ \mathcal{T}_r \circ \mathcal{T}_\theta$  as in Figure 3, where  $\mathcal{T}_\theta : z \in \mathbb{R}^{d-1} \mapsto \theta \in U_\theta^{d-1}$  is any diffeomorphism to  $d$ -spherical angles,  $\mathcal{T}_r : \theta \in U_\theta^{d-1} \mapsto [\theta, r(\theta)] \in U_\theta^{d-1} \times \mathbb{R}_{>0}$  a transformation as in Theorem 1 with  $r : \theta \in U_\theta^{d-1} \mapsto r \in \mathbb{R}_{>0}$  being differentiable, and  $\mathcal{T}_{s \rightarrow c} : [\theta, r(\theta)]^T \in U_\theta^{d-1} \times \mathbb{R}_{>0} \mapsto x \in \mathbb{R}^d$  the  $d$ -spherical to Cartesian transformation as in Definition 2.

Then, the Jacobian determinant of the full transformation  $\mathcal{T}$  is equal to

$$\det J_{\mathcal{T}} = \det J_{\mathcal{T}_\theta} \det J_{\mathcal{T}_{s \rightarrow c}} \|(J_{\mathcal{T}_{s \rightarrow c}}^T)^{-1} y\|_F, \quad (6)$$

where  $y := [-\nabla_\theta r(\theta), 1]^T$  and  $\|\cdot\|_F$  is the Frobenius norm. Relevantly, the Jacobian determinant in Eq. (6) can still be computed efficiently in quadratic time.

*Proof.* We start the proof by noting that the transformation  $\mathcal{T} := \mathcal{T}_{s \rightarrow c} \circ \mathcal{T}_r \circ \mathcal{T}_\theta$  is injective because  $\mathcal{T}_\theta$  is bijective,  $\mathcal{T}_r$  is injective because of Theorem 1 and  $\mathcal{T}_{s \rightarrow c}$  is also injective. Since the Jacobian matrix  $J_{\mathcal{T}} \in \mathbb{R}^{d \times d-1}$  is not squared, we cannot use the usual property of bijections in Eq. (1). Instead, we use the definition of Jacobian determinant for injective functions in Eq. (2):

$$\det J_{\mathcal{T}} = \sqrt{\det(J_{\mathcal{T}}^T J_{\mathcal{T}})} = \sqrt{\det\left(\left(J_{\mathcal{T}_{s \rightarrow c}} J_{\mathcal{T}_r} J_{\mathcal{T}_\theta}\right)^T \left(J_{\mathcal{T}_{s \rightarrow c}} J_{\mathcal{T}_r} J_{\mathcal{T}_\theta}\right)\right)}, \quad (20)$$

where  $J_{\mathcal{T}_r} \in \mathbb{R}^{d \times d-1}$  and  $J_{\mathcal{T}_{s \rightarrow c}} \in \mathbb{R}^{d \times d}$ . According to Remark 1 we can now show that we can factor out the Jacobian determinant of  $\mathcal{T}_\theta$ , i.e. the bijection that precedes the dimensional inflation step with  $\mathcal{T}_r$ :

$$\det J_{\mathcal{T}} = \det J_{\mathcal{T}_\theta} \det J_{\mathcal{T}_{s \rightarrow c} \circ \mathcal{T}_r} = \det J_{\mathcal{T}_\theta} \sqrt{\det\left(\left(J_{\mathcal{T}_{s \rightarrow c}} J_{\mathcal{T}_r}\right)^T \left(J_{\mathcal{T}_{s \rightarrow c}} J_{\mathcal{T}_r}\right)\right)}. \quad (21)$$

The term  $\det J_{\mathcal{T}_\theta}$  is the standard Jacobian determinant for bijective layers and can be computed efficiently. We are then left to compute  $\det J_{\mathcal{T}_{s \rightarrow c} \circ \mathcal{T}_r}$ . Similarly to the proof of Theorem (1), we now consider the matrix  $\tilde{J}_{\mathcal{T}_r} := [J_{\mathcal{T}_r} \mathbf{0}_{d \times 1}] \in \mathbb{R}^{d \times d}$  and substitute the determinant with the pseudo-determinant:

$$\det J_{\mathcal{T}_{s \rightarrow c} \circ \mathcal{T}_r} = \sqrt{\det\left(J_{\mathcal{T}_r}^T J^* J_{\mathcal{T}_r}\right)} = \sqrt{\text{Det}\left(\tilde{J}_{\mathcal{T}_r}^T J^* \tilde{J}_{\mathcal{T}_r}\right)}, \quad (22)$$

where  $J^* := J_{\mathcal{T}_s \rightarrow c}^T J_{\mathcal{T}_s \rightarrow c} \in \mathbb{R}^{d \times d}$ . With  $\text{Det}$  we denote the pseudo-determinant, which is defined as the product of all non-zero eigenvalues. The second equality follows from the fact that  $J_{\mathcal{T}_r}^T J^* J_{\mathcal{T}_r}$  and  $\tilde{J}_{\mathcal{T}_r}^T J^* \tilde{J}_{\mathcal{T}_r}$  have the same spectrum up to zero eigenvalues, so the determinant of the former coincides with the pseudo-determinant of the latter (by definition). To see that they share the same spectrum up to one zero eigenvalue, consider the explicit structure of the matrix product:

$$\tilde{J}_{\mathcal{T}_r}^T J^* \tilde{J}_{\mathcal{T}_r} = \begin{bmatrix} J_{\mathcal{T}_r}^T J^* J_{\mathcal{T}_r} & \mathbf{0}_{d-1 \times 1} \\ \mathbf{0}_{1 \times d-1} & 0 \end{bmatrix}. \quad (23)$$

Similarly to Theorem 1, the rest of the proof is based on the key observation that  $\tilde{J}_{\mathcal{T}_r}$  has rank  $d - 1$  or, equivalently, that its null space is one-dimensional. As a consequence, we can use Lemma 2 and re-write the pseudo-determinant in terms of the trace of the adjugate matrix:

$$\begin{aligned} \text{Det} \left( \tilde{J}_{\mathcal{T}_r}^T J^* \tilde{J}_{\mathcal{T}_r} \right) &= \text{Tr} \left( \text{adj} \left( \tilde{J}_{\mathcal{T}_r}^T J^* \tilde{J}_{\mathcal{T}_r} \right) \right) \\ &= \text{Tr} \left( \text{adj} \left( \tilde{J}_{\mathcal{T}_r}^T \right) \text{adj} \left( J^* \right) \text{adj} \left( \tilde{J}_{\mathcal{T}_r} \right) \right) \\ &= \det \left( J^* \right) \text{Tr} \left( \text{adj} \left( \tilde{J}_{\mathcal{T}_r} \right) \left( J^* \right)^{-1} \text{adj} \left( \tilde{J}_{\mathcal{T}_r}^T \right) \right). \end{aligned} \quad (24)$$

In the second equality we used the property that  $\text{adj}(AB) = \text{adj}(B) \text{adj}(A)$  for any  $A, B \in \mathbb{R}^{d \times d}$ , which easily generalizes to  $\text{adj}(ABC) = \text{adj}(C) \text{adj}(B) \text{adj}(A)$ . Lastly, if  $A$  is invertible,  $\text{adj}(A) = \det(A)A^{-1}$ . In this case  $J^* = J_{\mathcal{T}_s \rightarrow c}^T J_{\mathcal{T}_s \rightarrow c}$  has full rank and is thus invertible. Since the trace is a linear operator we can take out  $\det(J^*)$ , which is a constant.

Since  $\tilde{J}_{\mathcal{T}_r}$  has rank  $d - 1$ , its nullspace is one dimensional and we can pick  $x \in \mathbb{R}^d \mid \tilde{J}_{\mathcal{T}_r} x = 0$  to span the entire nullspace. The same holds for  $\tilde{J}_{\mathcal{T}_r}^T$ , or equivalently for the left nullspace of  $J_{\mathcal{T}_r}$ , and we can pick  $y \in \mathbb{R}^d \mid \tilde{J}_{\mathcal{T}_r}^T y = 0$ . We can easily compute  $x$  and  $y$  by looking at the structure of  $\tilde{J}_{\mathcal{T}_r}$ :

$$\tilde{J}_{\mathcal{T}_r} = \begin{bmatrix} 1 & 0 & \cdots & 0 & 0 \\ 0 & 1 & & & 0 \\ \vdots & & \ddots & & \vdots \\ 0 & & & 1 & 0 \\ \frac{\partial r}{\partial \theta_1} & \frac{\partial r}{\partial \theta_2} & \cdots & \frac{\partial r}{\partial \theta_{d-1}} & 0 \end{bmatrix} \quad x := \begin{bmatrix} 0 \\ 0 \\ \vdots \\ 0 \\ 1 \end{bmatrix} \quad y := \begin{bmatrix} -\frac{\partial r}{\partial \theta_1} \\ -\frac{\partial r}{\partial \theta_2} \\ \cdots \\ -\frac{\partial r}{\partial \theta_{d-1}} \\ 1 \end{bmatrix}. \quad (25)$$

We now make use of Lemma 1 for  $\tilde{J}_{\mathcal{T}_r}$ , which gives us

$$\text{adj}(\tilde{J}_{\mathcal{T}_r}) = \frac{\text{Det}(\tilde{J}_{\mathcal{T}_r})}{y^T x} x y^T. \quad (26)$$

We can now substitute Eq. (26) in Eq. (24):

$$\begin{aligned} \text{Det} \left( \tilde{J}_{\mathcal{T}_r}^T J^* \tilde{J}_{\mathcal{T}_r} \right) &= \det \left( J^* \right) \frac{\text{Det}(\tilde{J}_{\mathcal{T}_r})^2}{(y^T x)^2} \text{Tr} \left( x y^T \left( J^* \right)^{-1} y x^T \right) \\ &= \det \left( J_{\mathcal{T}_s \rightarrow c}^T J_{\mathcal{T}_s \rightarrow c} \right) \frac{\text{Det}(\tilde{J}_{\mathcal{T}_r})^2 x^T x}{(y^T x)^2} \text{Tr} \left( y^T \left( J^* \right)^{-1} y \right) \\ &= \det \left( J_{\mathcal{T}_s \rightarrow c} \right)^2 \left\| \left( J_{\mathcal{T}_s \rightarrow c}^T \right)^{-1} y \right\|_F^2. \end{aligned} \quad (27)$$

In the first equality we used the fact that  $\text{adj}(A^T) = \text{adj}(A)^T$  and we factored out  $\text{Det}(\tilde{J}_{\mathcal{T}_r})^2$  and  $(y^T x)^2$ , which are constants. In the second equality we used the cyclic property of the trace and factored out  $x^T x$ . Lastly, we substituted the numerical values  $\text{Det}(\tilde{J}_{\mathcal{T}_r}) = 1$ ,  $y^T x = 1$  and  $x^T x = 1$  and used the property that  $\text{Tr}(A^T A) = \|A\|_F^2$ , with  $\|\cdot\|_F$  being the Frobenius norm.

We can now analyze the time complexity required to evaluate Eq. (6). The Jacobian determinant for spherical to Cartesian coordinates is known Muleshkov and Nguyen [2016]

$$\det J_{s \rightarrow c} = (-)^{d-1} r^{d-1} \prod_{k=1}^{d-2} \sin^{d-k-1} \theta_k \quad (28)$$



and can be computed efficiently in  $O(d)$  time. Therefore, we only need to show that also  $w = (J_{\mathcal{T}_{s \rightarrow c}}^T)^{-1} y$  can be computed efficiently. Solving the full linear system would require a complexity of  $O(d^3)$ . However, we can exploit the almost-triangular structure of

$$J_{\mathcal{T}_{s \rightarrow c}}^T = \begin{bmatrix} \frac{\partial x_1}{\partial \theta_1} & \frac{\partial x_2}{\partial \theta_1} & \cdots & \frac{\partial x_{d-1}}{\partial \theta_1} & \frac{\partial x_d}{\partial \theta_1} \\ 0 & \frac{\partial x_2}{\partial \theta_2} & \cdots & \frac{\partial x_{d-1}}{\partial \theta_2} & \frac{\partial x_d}{\partial \theta_2} \\ \vdots & & \ddots & & \vdots \\ 0 & 0 & & \frac{\partial x_{d-1}}{\partial \theta_{d-1}} & \frac{\partial x_d}{\partial \theta_{d-1}} \\ \frac{\partial x_1}{\partial r} & \frac{\partial x_2}{\partial r} & \cdots & \frac{\partial x_{d-1}}{\partial r} & \frac{\partial x_d}{\partial r} \end{bmatrix} \quad (29)$$

to solve the linear system in  $O(d^2)$ . One possibility is to perform one step of Gaussian elimination, which requires  $O(d)$ , and make the linear system triangular. The resulting triangular system can be solved in  $O(d^2)$ . Alternatively, we can invert  $J_{\mathcal{T}_{s \rightarrow c}}^T$  in  $O(d^2)$  by using the Sherman-Morrison formula (or rank-one update inverse). In the latter case,  $J_{\mathcal{T}_{s \rightarrow c}}^T$  can be re-written as the sum of an upper triangular matrix  $U$  and a rank-1 matrix  $uv^T$  as

$$U = \begin{bmatrix} \frac{\partial x_1}{\partial \theta_1} & \frac{\partial x_2}{\partial \theta_1} & \cdots & \frac{\partial x_{d-1}}{\partial \theta_1} & \frac{\partial x_d}{\partial \theta_1} \\ 0 & \frac{\partial x_2}{\partial \theta_2} & \cdots & \frac{\partial x_{d-1}}{\partial \theta_2} & \frac{\partial x_d}{\partial \theta_2} \\ \vdots & & \ddots & & \vdots \\ 0 & 0 & & \frac{\partial x_{d-1}}{\partial \theta_{d-1}} & \frac{\partial x_d}{\partial \theta_{d-1}} \\ 0 & 0 & \cdots & 0 & \frac{\partial x_d}{\partial r} \end{bmatrix} \quad u := \begin{bmatrix} 0 \\ 0 \\ \vdots \\ 0 \\ 1 \end{bmatrix} \quad v := \begin{bmatrix} \frac{\partial x_1}{\partial r} \\ \frac{\partial x_2}{\partial r} \\ \vdots \\ \frac{\partial x_{d-1}}{\partial r} \\ 0 \end{bmatrix}. \quad (30)$$

We can now compute the inverse of  $J_{\mathcal{T}_{s \rightarrow c}}^T$  by only inverting the triangular matrix  $U$ :

$$(J_{\mathcal{T}_{s \rightarrow c}}^T)^{-1} = (U + uv^T)^{-1} = U^{-1} - \frac{U^{-1}uv^T U^{-1}}{1 + v^T U^{-1}u}. \quad (31)$$

Since  $U$  is upper triangular, its inverse can be computed through back substitution in  $O(d^2)$ . Note that we can compute  $J_{\mathcal{T}_{s \rightarrow c}}$  very efficiently and analytically (see Eq. (33)), without requiring autograd computations. Overall, the determinant of the full transformation  $\mathcal{T}$  can be obtained as

$$\det J_{\mathcal{T}} = \det J_{\mathcal{T}_\theta} \det (J_{\mathcal{T}_{s \rightarrow c}})^2 \|(J_{\mathcal{T}_{s \rightarrow c}}^T)^{-1} y\|_F^2 \quad (32)$$

and can be computed efficiently in  $O(d^2)$ . ■

## A.5 Implementation details

**Implementation of injective flows for star-like manifolds** We provide some details about the implementation of the proposed injective flows and particularly for star-like manifolds in Cartesian coordinates as in Figure 3. We implement the layers in three steps:

- **bijection layers  $\mathcal{T}_z$  and  $\mathcal{T}_\theta$ .** The first bijection  $\mathcal{T}_z : z \mapsto z'$  consists of arbitrary (conditional) bijective layers conditioned on the parameter  $\lambda$ . The conditioning is realized with an expressive Residual network. Then,  $\mathcal{T}_\theta : z' \mapsto \theta$  maps the transformed  $z'$  into spherical angles  $\theta \in U_\theta^{d-1}$ . This last transformation is also a bijection that can be implemented with an element-wise non linear activation like Sigmoid (hence diagonal Jacobian). Otherwise, one could use a base distribution which is already defined on the  $d - 1$  spherical angles and use a bijective transformation that transforms  $\theta$  within their domain  $U_\theta^{d-1}$  as  $\mathcal{T}_{\text{circ}} : \theta \in U_\theta^{d-1} \mapsto \theta' \in U_\theta^{d-1}$ . We use the circular bijective layers proposed by Rezende et al. [2020] because they allow to nicely integrate the boundary conditions arising from the use of spherical coordinates. In particular, circular layers automatically enforce continuity of the density at the boundary of the domain. Circular layers require the base distribution to be defined on  $U_\theta^{d-1}$ . In practice, we use the distribution of spherical angles, which results in uniform points on the  $d - 1$  dimensional sphere, and can be implemented efficiently. We use the implementation of circular layers provided in Stimper et al. [2023].

- **injective layer**  $\mathcal{T}_r$ . The injective step  $\mathcal{T}_r : \boldsymbol{\theta} \mapsto [\boldsymbol{\theta}, r(\boldsymbol{\theta})]^T$  only consists in padding the spherical angles with some specified radius function  $r(\boldsymbol{\theta})$ . The specific expression for the radius function depends on the manifold considered and is detailed in Eq. (34) and Eq. (35) for the  $l_p$  (pseudo-) norm ball and for the probabilistic simplex  $\mathcal{C}^d$ , respectively. In variational inference settings  $\mathcal{T}_r$  is not a learnable transformation. In density estimation tasks, if we assume the data was generated from a  $d - 1$  star-like manifold,  $r(\boldsymbol{\theta})$  can be implemented with a neural network and made learnable. This would allow to learn the manifold and would provide with a very practical global parameterization.
- **bijective layer**  $\mathcal{T}_{s \rightarrow c}$ : the bijective layer  $\mathcal{T}_{s \rightarrow c} : [\boldsymbol{\theta}, r(\boldsymbol{\theta})] \mapsto \boldsymbol{x}$  simply implements the spherical to Cartesian transformation in Eq. (5), which is a bijection and can be implemented efficiently.  $\mathcal{T}_{s \rightarrow c}$  is not a trainable transformation.

For the implementation we rely on the (conditional) normalizing flow library *FlowConductor*<sup>1</sup>, which was introduced in Negri et al. [2023] and Torres et al. [2024].

**Efficient implementation of the Jacobian of spherical to Cartesian transformation** In order to compute the determinant in Eq. (6) we need to compute the Jacobian determinant of the transformation from spherical to Cartesian coordinates  $J_{\mathcal{T}_{s \rightarrow c}}^T$ . By looking at the definition of the coordinate transformation in Eq. (5), we can easily derive the following expression:

$$J_{\mathcal{T}_{s \rightarrow c}}^T = \begin{bmatrix} -rs_1 & rc_1c_2 & \cdots & rc_1s_2 \cdots s_{d-2}c_{d-1} & rc_1s_2 \cdots s_{d-2}s_{d-1} \\ 0 & -rs_1s_2 & \cdots & rs_1c_2 \cdots s_{d-2}c_{d-1} & rs_1c_2 \cdots s_{d-2}s_{d-1} \\ 0 & 0 & \ddots & \vdots & \vdots \\ 0 & 0 & \cdots & -rs_1s_2 \cdots s_{d-2}s_{d-1} & s_1s_2 \cdots s_{d-2}c_{d-1} \\ c_1 & s_1c_2 & \cdots & s_1s_2 \cdots s_{d-2}c_{d-1} & s_1s_2 \cdots s_{d-2}s_{d-1} \end{bmatrix} \quad (33)$$

where we used the shorthand  $s_i = \sin \theta_i$  and  $c_i = \cos \theta_i$ . This allows to compute  $J_{\mathcal{T}_{s \rightarrow c}}^T$  extremely efficiently without requiring to use autograd computations and results in a significant speed up.

**Parametrization of  $l_p$  (pseudo-) norm balls** Here we show how to parametrize the  $l_p$  (pseudo-) norm balls in spherical coordinates. Let the  $l_p$  (pseudo-) norm of  $\boldsymbol{x} \in \mathbb{R}^d$  be defined as  $\|\boldsymbol{x}\|_p = (|x_1|^p + \dots + |x_d|^p)^{1/p}$  with  $p > 0$ . We consider now the manifold defined by  $\|\boldsymbol{x}\|_p = t$  for some  $k \in \mathbb{R}_{>0}$ . If we write  $\boldsymbol{x}$  in spherical coordinates according to Eq. (5), we can take the radius  $r$  outside of the norm and express it as a function of the  $d - 1$  spherical angles as:

$$r(\theta_1, \dots, \theta_{d-1}) = \frac{t}{\left( |\cos \theta_1|^p + \sum_{i=2}^{d-1} \left| \cos \theta_i \prod_{k=1}^{i-1} \sin \theta_k \right|^p + \left| \prod_{k=1}^{d-1} \sin \theta_k \right|^p \right)^{1/p}}. \quad (34)$$

We can use this expression to parametrize the  $l_p$  norm balls with the proposed injective flows. Similarly, we can also parametrize the probabilistic simplex  $\mathcal{C}^d$ . To see this consider the  $l_1$  norm ball  $\|\boldsymbol{x}\|_1 = |x_1| + \dots + |x_d|$ . If we restrict the domain to the positive quadrant  $\boldsymbol{x} \in \mathbb{R}_{\geq 0}^d$  and set the norm to 1, the resulting manifold is defined as  $\|\boldsymbol{x}\|_1 = x_1 + \dots + x_d = 1$  and coincides with  $\mathcal{C}^d$ . The radius is then parametrized by

$$r(\theta_1, \dots, \theta_{d-1}) = \frac{1}{\cos \theta_1 + \sum_{i=2}^{d-1} \cos \theta_i \prod_{k=1}^{i-1} \sin \theta_k + \prod_{k=1}^{d-1} \sin \theta_k} \quad \text{with } \theta_i \in [0, \pi/2] \forall i, \quad (35)$$

where the constraint on the angles enforces  $\boldsymbol{x} \in \mathbb{R}_{\geq 0}^d$ . Note that it is straightforward to analytically derive the expression for the partial derivatives  $\frac{\partial r}{\partial \theta_i}$  in Eq. (35). This makes the computation of  $y$  in Eq.(6) more efficient than computing the gradients with autograd and results in a speed up.

<sup>1</sup><https://github.com/FabricioArendTorres/FlowConductor>

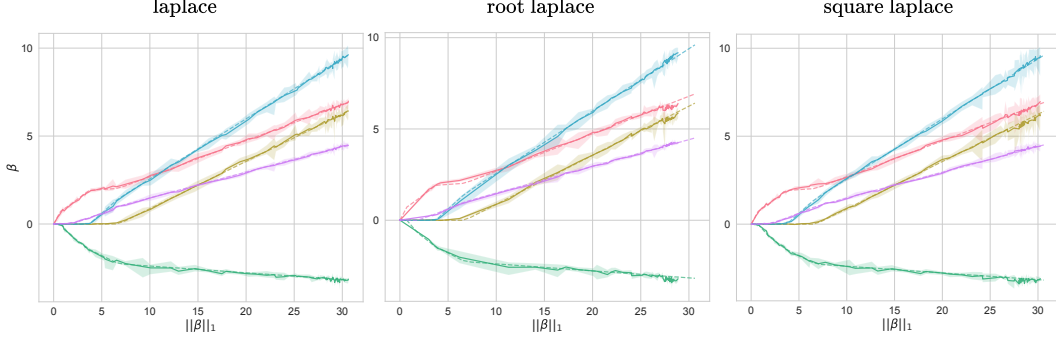


Figure 7: MAP solution for Laplace prior, root Laplace and square Laplace, which are all monotonic transformation of the Laplace distribution. The MAP solution paths coincide.

## A.6 Applications: further details

### A.6.1 Architecture

We use two different architectures. One is for standard NFs that we use for the subjective penalized likelihood regression problem. The other architecture is the injective flow that is used for the objective Bayes version of the regression problem and the portfolio diversification application.

**Standard NF** It consists of a normal distribution as base distribution. Then we use 5 blocks of permutation transformation, a sum of Sigmoids layer [Torres et al., 2024] and an activation norm. The sum of Sigmoid layer consists each of 30 individual Sigmoid functions in three blocks.

**Injective flows** The base distribution is either the probabilistic simplex or the complete  $\|\beta\|_1 = 1$  depending on the application. We follow this with again 5 layers of the circular bijective layers [Rezende et al., 2020], each consisting of three blocks with 8 bins. At the end these values are mapped to Cartesian coordinates with the proposed dimensionality inflation step.

### A.6.2 Training

Both the standard NFs and the injective flows are trained by minimizing the reverse KL divergence with respect to the (unnormalized) target density  $p(\mathbf{x})$ :

$$q_{\theta^*}(\mathbf{x}) = \arg \min_{\theta \in \Theta} \text{KL}(q_{\theta}(\mathbf{x}) || p(\mathbf{x})) = \arg \min_{\theta \in \Theta} \mathbb{E}_{\mathbf{x} \sim q_{\theta}} \left[ \log \frac{q_{\theta}(\mathbf{x})}{p(\mathbf{x})} \right]. \quad (36)$$

We optimize the reverse KL divergence using Adam [Kingma and Ba, 2017] as optimizer with default parameters. Notably, all trained flows converged in a matter of minutes on a standard commercial GPU (RTX2080Ti in our specific case).

### A.6.3 Penalized likelihood regression

In the next paragraph we provide further details on the experiment introduced in Section 5.1, which involves the penalized likelihood model defined in Eq. (7).

**Synthetic dataset creation** The synthetic regression dataset is created by sampling  $X^*$  from a 5 dimensional Wishart distribution  $W_5(7, I)$ . The response variable  $y$  is then created by  $X^* \beta^* + \epsilon$  where  $\beta^*$  is standard normal distributed and  $\epsilon$  is normal distributed with zero mean and a standard deviation of 4.0.

**Subjective Bayes** The subjective Bayes relies on a prior  $p(\beta|\lambda)$ . The Laplace prior is given by

$$p_{lap}(\beta|\lambda) \propto \prod_i \exp\{-\lambda|\beta_i|^p\}. \quad (37)$$

The two other test priors are  $p_{sq}(\beta|\lambda) \propto p_{lap}(\beta|\lambda)^2$  and  $p_{rt}(\beta|\lambda) \propto p_{lap}(\beta|\lambda)^{1/2}$ . Any monotonic transformation may change the  $\lambda$ -axis but leave the MAP solution path unchanged. This can be

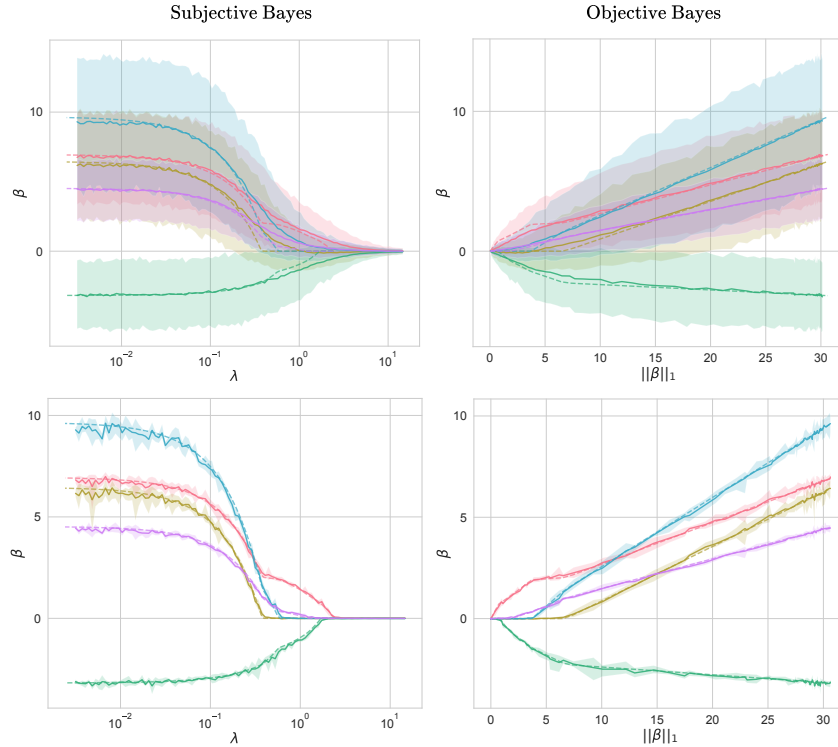


Figure 8: Solution paths for subjective prior as a function of  $\lambda$ , and objective priors, as a function of the norm  $\|\beta\|_1$ . Below we report the solution paths in the MAP limit.

seen in Figure 7 where we show the MAP solution path for different subjective priors. For this visualization we reparameterize the axis such that the  $\lambda$ -axis is transformed into a  $\|\beta\|_1$ -axis. This makes clear that the solution paths are equivalent.

**Objective Bayes** The objective Bayes approach circumvents the definition of  $p(\beta|\lambda)$ . The flow is directly defined on the manifolds coinciding with the contour lines of  $p(\beta|\lambda)$ . As such, samples from the posterior all share a chosen norm value  $\|\beta\|_1 = k$ . Figure 8 highlights the different parametrizations of the subjective and objective approach.

**Portfolio optimization** In portfolio optimization the cumulative return is often of interest. Figure 9 shows the effect of the different priors on the cumulative return. The sparser priors lead to a slightly wider distribution of the return. In this example, this leads to the target index being a closely matched by some of the posterior samples, where the samples of the uniform prior seem to be further away from the target index in some parts of the time interval. The bottom row of the Figure 9 further shows the sampled sparsity patterns. These show that the sparse priors can lead to significantly different mixtures with similar data fitting quality.

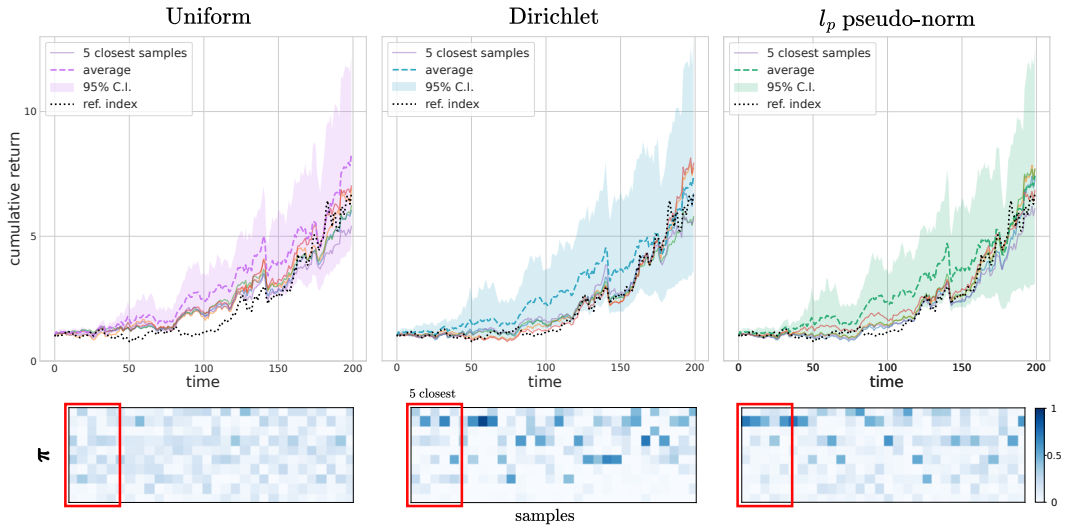


Figure 9: Cumulative return as a function of time. We plot 95% posterior C.I. with the uniform prior, Dirichlet prior and  $l_p$ -norm prior. We also plot the 5 samples that are the closest to the ground truth cumulative return. In the bottom panel we visualize the weight samples as a heatmap to highlight sparsity patterns.